

Wolfram Schmidt\*, Swen Grossmann, Eric Bohne, Peter Behrens, Klaus-Peter Schmitz

# Radiopacity of Implants – Micro-CT Compared to Standardized Medical Imaging

<https://doi.org/10.1515/cdbme-2025-0136>

**Abstract:** Radiopacity is an important prerequisite for X-ray visibility of implants. Existing standards refer to the use of X-ray systems for medical imaging. Micro Computed Tomography ( $\mu$ CT) technology is available with high resolution imaging. Experimental studies should verify the comparability of radiopacity results with respect to filtering, image resolution and composition of reference samples. The study yielded that radiopacity can be measured with differing equipment. Advantageous for  $\mu$ CT are high resolution, flat field correction and avoidance of radiation protection measures when using full protection devices. However, the results cannot match the requirements of related standards, because sample distance and simulation of body scattering are limited. Both might be important when using the data for assessment of X-ray visibility in clinical settings.

**Keywords:** Biomedical Engineering, Medical Imaging, Radiopacity, Standardization, Surgical Implants

## 1 Introduction

Radiographic visibility of implantable medical devices is important for monitoring implantation, therapy success, and device performance. It is determined among other parameters by image resolution and noise with radiopacity as a basic requirement. Several standards for medical implants require assessment of device visibility [1][2].

Existing standards for measurement of radiopacity refer to the use of X-ray systems for medical imaging [3][4]. However, and in particular in research and development of materials and devices, research equipment such as  $\mu$ CT could also provide meaningful results. Such research related to

improved radiopacity of low-weight metallic implants, polymers or catheters is common [5][6][7].

It is known that the maximum X-ray energy as well as the energy spectrum may also impact radiopacity. Therefore, the defined setting of  $80 \pm 5$  kV is required [4]. Filtering will reduce the contribution of low energy rays to the image and at the same time reduces radiation dose. This effect is included in the study by using two different filter options.

Micro Computer Tomography ( $\mu$ CT) technology is a high resolution imaging modality. Experimental studies will be presented to verify the comparability of  $\mu$ CT results to those of testing by standardized medical imaging with respect to filtering, resolution and composition of reference samples.

## 2 Material and Methods

### 2.1 Medical Imaging Setup

Medical imaging was conducted with the digital Radiography device Fuji FXR Multisuite consisting of X-ray bush (Siemens, type SV 150/40/80C-100), Fujifilm Digital Radiography Device and Flat Panel Sensor (Fujifilm FDR D-EVO II, type C35, 14 x 17", 2836 x 2336 px, pixel pitch 150  $\mu$ m) as digital detector. A 3.0 mm Al filter is integrated in the aperture system and filter unit. The scattering phantom was a 150 mm thick PMMA block composed of PMMA slices. A digital negative image is provided for analysis.

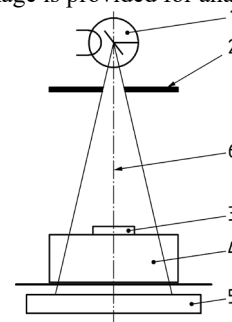


**Figure 1:** Imaging setup for the determination of X-ray contrast according to DIN 13273-7:2020-12 (1 – X-ray bush, 2 – aperture system, 3 – test samples, 4 – scattering phantom, 5 – detector, 6 – central beam) [4]

\*Corresponding author: **Wolfram Schmidt:** Institute for Biomedical Engineering, University Medical Center Rostock, Rostock, F.-Barnewitz-Str. 4, 18119 Rostock-Warnemünde, Germany, e-mail: wolfram.schmidt@uni-rostock.de

**Swen Grossmann, Eric Bohne, Peter Behrens, Klaus-Peter Schmitz:** Institute for ImplantTechnology and Biomaterials – IIB e.V., Rostock-Warnemünde, Germany

## 2.2 Micro Computer Tomography

For comparison with medical imaging, the  $\mu$ CT (SKYSCAN 1273, Bruker) was used (fixed distance source - sensor 500 mm, camera resolution 74.8  $\mu$ m). Adjusting the distance between test sample and source, a resolution of 25  $\mu$ m per pixel was achieved. For comparison absorption of step wedges was also tested at about half resolution (51  $\mu$ m/pixel).

For assessment of radiopacity one 2D image was taken, without complete 3D scan. Imaging was performed without and with 1 mm aluminium filter. The imaging parameters were set to: 80 kV, 50  $\mu$ A and 450 ms (no filter) or 605 ms (1 mm Al filter). A digital positive image is provided and available for analysis according to [4].

## 2.3 Test samples

Reference samples were 1 – 10 mm thick step wedges (99.5% Al compared to AlCuMg alloy, fitted to  $\mu$ CT dimensions). A rod (diameter 3 mm) was used as test sample for quantitative assessment. It consisted of 99.5% Al and thus should have the same radiopacity as the 3 mm thick reference sample made from the same material.

Several commercially available implants were included to demonstrate radiopacity of implants for different medical indications (see Table 1).

**Table 1:** List of medical implants used for comparative measurement of radiopacity

Test sample	Type	Dimension [mm]	Manufacturer
Peripheral Stent	Absolute Pro	6 x 40	Abbott Vascular
Peripheral Stent	Sinus Carotid	6 x 40	Optimed
Coronary Drug Eluting Stent System	Coroflex ISAR	3.0 x 16	B.Braun Melsungen AG
Coronary Drug Eluting Stent System	XIENCE Sierra	3.0 x 15	Abbott Vascular
Gold Fiducial Marker	VISICOIL	0.35 x 5	ILUMARK
Gold Fiducial Marker	VISICOIL	0.35 x 10	ILUMARK

The peripheral stents are self-expanding Nitinol stents with the Absolute Pro having additional radiopaque markers at the distal and proximal ends. The coronary stent systems consist of drug-eluting CoCr stents crimped on balloon catheters. They exhibit markers to indicate the distal and proximal end of the stents position. The gold fiducial markers

consist of tightly wound gold wires resulting in very flexible markers for indication of treatment sites, i.e. during radiation therapy.

## 2.4 Analysis of radiopacity

For quantitative assessment the greyscale values of the images (0 to 255) were extracted in the region of the test samples and in the region of the immediate adjacent area (background). Furthermore, the contrast of the Al step wedge was determined according to [4], sect. 7.2.3.

The Al equivalent of the test samples (in mmAl) was calculated acc. to [4], sect. 7.2.4., by assigning intermediate greyscale values to the related Al thickness of the step wedge by linear interpolation.

## 3 Results

The resulting image taken with the medical imaging setup is shown in Figure 2. The obtained radiopacity in terms of Al equivalent (in mmAl) is shown in Figure 3.

$\mu$ CT imaging provided highly reproducible images for the different parameters. Examples are given for step wedges consisting of 99.5% Al and AlCuMg alloy, as well as the 99.5% Al step wedge with the Nitinol stent Absolute Pro, imaged without filter and using a 1 mm Al filter (see Figure 4).

The radiopacity of the smaller AlCuMg alloy step wedge was higher than that of 99.5% aluminium. Filtering also provides visible grayscale differences.

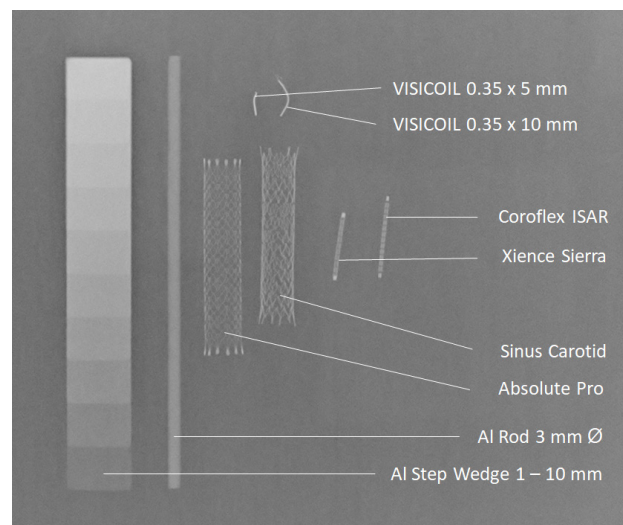


**Figure 2:** X-ray image of test and reference samples (Fuji FXR Multisuite, 81 kV, 6.16 mAs), Al step wedge 1 – 10 mm, made from 99.5% Al

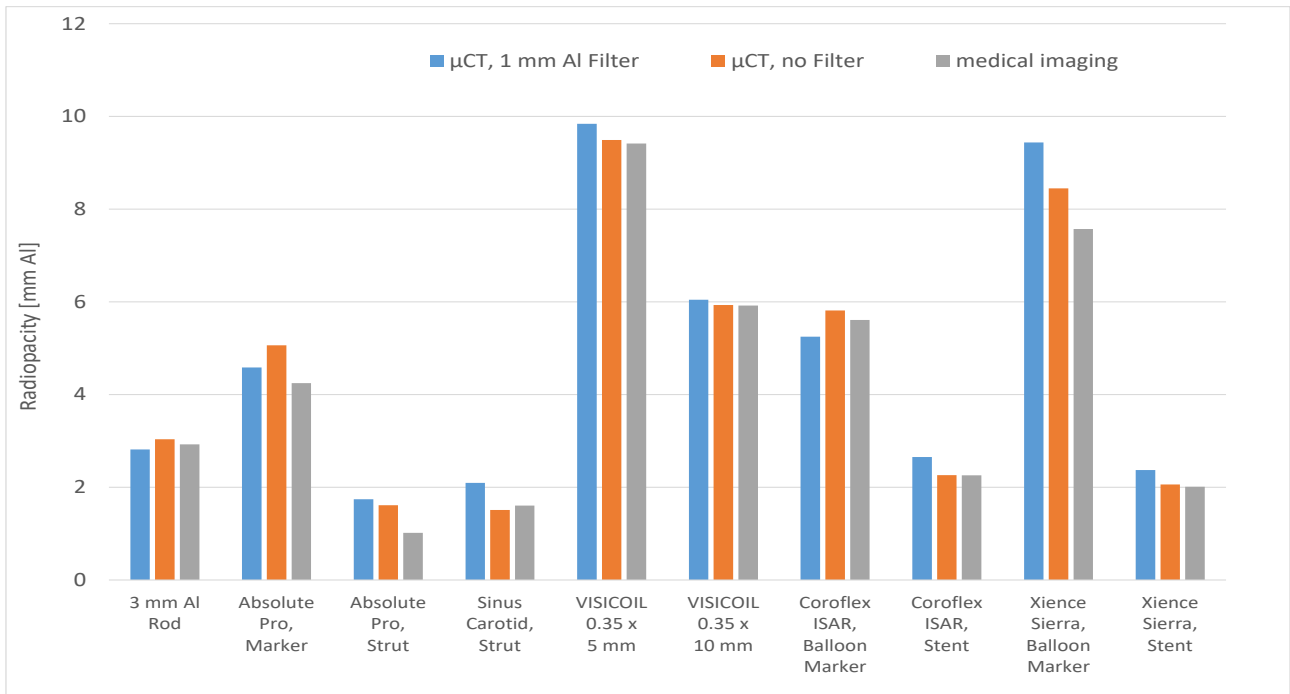


**Figure 3:** Radiopacity of test samples (in mmAl), derived from  $\mu$ CT images filtered by 1 mm Al and unfiltered as well as medical imaging according to [4]

The systematic comparison of greyscale values from the two types of Al step wedges yielded differences depending on the Al alloy (AlCuMg vs. 99.5% Al, Figure 5) and filtering (Figure 6) but no differences for image resolution.

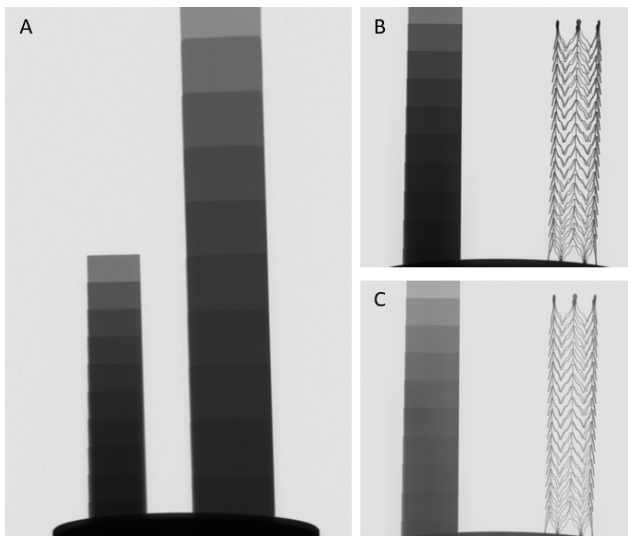


**Figure 4:**  $\mu$ CT Images of Al step wedges – A) AlCuMg (left) vs. 99.5% Al (right), both with identical thickness, resolution 51  $\mu$ m, B) AlCuMg step wedge and Nitinol stent Absolute Pro, unfiltered, C) AlCuMg step wedge and Nitinol stent Absolute Pro, filtered with 1 mm Al

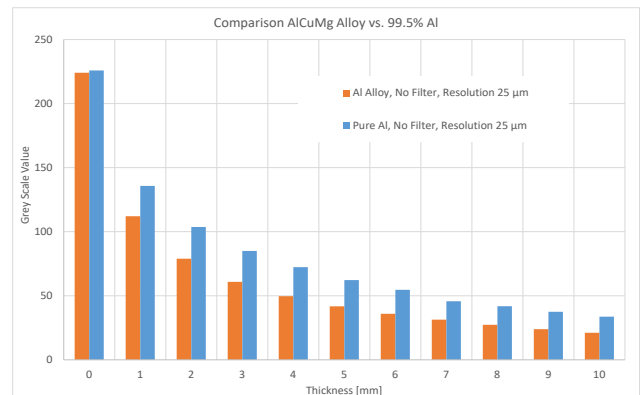


**Figure 5:** Greyscale values of step wedges 1 – 10 mm, 99.5% Al compared to AlCuMg alloy ( $\mu$ CT, 80 kV, resolution 25  $\mu$ m)

The greyscale values of the step wedges were reproducible ( $n=6$ , maximum SD = 0.33 or 1.1% @ 10 mm Al). Radiopacity from  $\mu$ CT yielded comparable results to medical imaging (Figure 3). Best agreement for the 3 mm Al rod was achieved with the unfiltered  $\mu$ CT scan (3.04 mm Al).

The high resolution of  $\mu$ CT imaging allows for the localization of small implant components such as stent struts or gold fiducial markers (Figure 7).

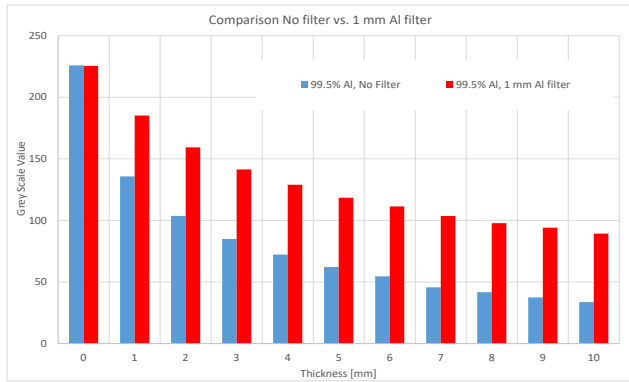


**Figure 6:** Greyscale values of step wedge 1 – 10 mm, 99.5% Al, unfiltered compared to filtered by 1 mm Al ( $\mu$ CT, 80 kV, resolution 25  $\mu$ m)

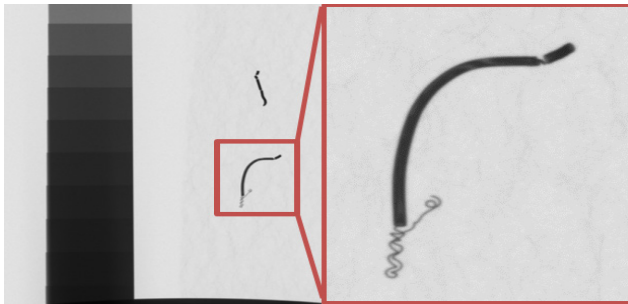


**Figure 7:** Gold fiducial markers with visible microstructure of wound wires, the resolution could be even higher when using a smaller Al reference ( $\mu$ CT, 80 kV, resolution 25  $\mu$ m)

## 4 Discussion

For both investigated imaging modalities, different absolute greyscale values were obtained. Filtering reduces contrast, provides less non-linear characteristics and enables more sensitive discrimination between different greyscale values over the entire range (0 to 10 mm Al, see Figure 6).

Furthermore, it was found that the requirement to use at least 99.5% Al as reference is very insightful when providing radiopacity data in terms of mmAl.

Considering the energy-dependent absorption and scattering of X-rays, filtering can have an impact on radiopacity depending on density and atomic number of the absorbing material, even at fixed maximum energy (80 keV). Some differences in Figure 3 may be caused by this effect, for example at the balloon markers.

The use of  $\mu$ CT equipment provides essential advantages like radiation protection, high image resolution, and flat-field correction. In medical imaging systems inhomogeneous images result from the heel effect of X-ray tube and anti-scatter grids, reducing the usable region of interest to the central beam.

A major challenge of  $\mu$ CT compared to medical imaging is the limited use of body mimicking phantoms. Scattering phantoms consisting of Al may be used [3]. This has less effect on

radiopacity but on assessment of visibility. Most device related standards do not distinguish properly between X-ray visibility and radiopacity.

## 5 Conclusion

Radiopacity can be measured with non-medical equipment. Advantageous are high resolution, flat field correction and radiation protection when using full protection  $\mu$ CT devices. However, the results cannot match requirements of standards, because sample distance and simulation of body scattering are limited. Both might be important when using the data for assessment of X-ray visibility in clinical settings.

## 6 Acknowledgements

The authors thank the Institute for Diagnostic and Interventional Radiology, Pediatric Radiology and Neuroradiology (Director: Prof. Dr. med. Marc-André Weber) at the University Medical Center Rostock for the opportunity to use the medical imaging equipment.

### Author Statement

Research funding: Financial support by the European Regional Development Fund (ERDF) and the European Social Fund (ESF) within the collaborative research between economy and science of the state Mecklenburg-Vorpommern is gratefully acknowledged. Conflict of interest: Authors state no conflict of interest. Informed consent: Not applicable. Ethical approval: Not applicable

## References

- [1] DIN EN ISO 10555-1:2024 Intravascular catheters - Sterile and single-use catheters - Part 1: General requirements (ISO 10555-1:2023)
- [2] DIN EN ISO 25539-2:2021-01 Cardiovascular implants - Endovascular devices - Part 2: Vascular stents (ISO 25539-2:2020)
- [3] ASTM F640-23 Standard Test Methods for Determining Radiopacity for Medical Use
- [4] DIN 13273-7:2020-12 Catheter for medical use - Part 7: Determination of the x-ray attenuation of catheters; requirements and testing
- [5] Kapadia Y, Jain V. (2018): Radiopacity of Dental Materials used for Imaging Guides in Implant Dentistry. In: *EC Dental Science* 17 (6).
- [6] Emonde CK; Eggers ME; Wichmann M; et al. (2024): Radiopacity Enhancements in Polymeric Implant Biomaterials: A Comprehensive Literature Review. In: *ACS biomaterials science & engineering* 10 (3), S. 1323–1334.
- [7] Jiang, YY; Jo YE; Woo JM; et al. (2017): In Vitro Quantification of the Radiopacity of Onyx during Embolization. In: *Neurointervention* 12 (1), S. 3–10